Influence of spatial resolution on susceptibility mapping of landslides: a case study of western Oregon.

Nicholas Hallahan and Rubini Mahalingam

Introduction

The USGS states that Oregon`s most devastating geologic hazard is landslides, with an annual repair cost exceeding $10 million. With the increase in population, it throws a significant threat for the loss of the lives as well which emphasizes on the pre disaster mitigation which could be broken down in different scales. One such important attempt is to map the susceptible zones based on previous datasets of landslides which helps in effective mitigation. It is witnessed that mass movements occur in the coastal regions of Oregon at irregular intervals with variable volume of material which leads to the importance of mapping landslide susceptibility (C. T. Lee et al., 2008).

GIS and remote sensing techniques have been proven to be very efficient for landslide hazard mapping which are influenced by many parameters such as slope, aspect, seismic activity, fault patterns, soil type, lithology, land use, and geomorphology (Dogami, 2010; GEO, 2009; Guzzetti, Carrara, Cardinali, & Reichenbach, 1999; Guzzetti, Reichenbach, Cardinali, Galli, & Ardizzone, 2005; Huete et al., 2002). Spatial and temporal resolutions contribute to the quality of the maps generated. Hence it is necessary to understand the effect of the resolution of the datasets which are widely used for susceptibility mapping. Such influences vary based on the type of the terrain it is applied.

The data processing involves multiple grid files, and the steps are iterative in order to make a comparison study among different cell sizes. To save time, it is more effective to write a batch processing script to automate the steps required to process our data.

Study area

Figure 1

Datasets

Landslide inventory is the most important data in the mapping process and has a high influence over the quality of the results. SLIDO (Statewide Landslide Information Database of Oregon Release 2)(William Burns, 2011) was collected from DOGAMI() which contains 20,000 point features representing past landslide occurrences . The inventory records include the flows, slides, falls, and the complexities that occurred between 1960-2011. The determinant factors include slope, aspect, slope roughness, TWI (Topographic Wetness Index) and NDVI (Normalized Differential Vegetative Index).

Determinant factors such as slope gradient, aspect, slope roughness, terrain roughness, distance from the streams, NDVI, land cover, distance from the faults and precipitation which

influence the slope stability conditions are processed in ArcGIS 10.0. Slope gradient, slope roughness, terrain roughness and aspect were derivatives of Advanced Space borne Thermal Emission and Reflection (ASTER) DEM with the cell size of 27 m. The file-geodatabase was used to store all the continuous layers and categorical layers namely lithology and land cover. ERDAS imagine 2010 model builder was used to generate the NDVI map from Landsat7 ETM + from the Near Infra-red and red bands

Generation of the data

Data	Software used	Techniques
Shape files	ArcGIS 10	Defining the projection
		Feature to Raster
Satellite images	ERDAS Imagine 2010	Mosaic
		Resampling
		Haze correction
		Subset and chip

Shape files	Satellite images	Reports
Unstable slope	GDEM	Geotechnical reports
SLIDO	Landsat ETM +	
Lithology		

Feature to raster files	Derivatives of satellite images
Lithology	Slope
Land use and land cover	Aspect
	NDVI
	Precipitation

Methodology

In the frequency ratio probability model, which is used in landslide hazard prediction, each pixel is joint conditional probability that the pixel will be affected by a similar event subject to information from the spatial information at that pixel (Chung and Fabbri,1999). In other words, it is a probability of occurrence to nonoccurrence for a given parameter. In order to define a model to predict an occurrence of an event, it is assumed that it will happen again based on its related factors and the conditions which caused landslides in past ((C. T. Lee et al., 2008; S. Lee & Min, 2001; S. Lee & Sambath, 2006; Saro Lee, Choi, & Woo, 2004; Lobo, 2007; Madin & Burns, 2006; Marcus, 2008; Nandi & Shakoor, 2010)) . Frequency Ratio(FR) is computed by adding all the factors in each size in each factor for the landslides divided by the total pixels in the same bin. If the factor is greater than 1 for each bin, then the autocorrelation is strong between them. Negative indicates that it is less related. For example, FR is -1.45 for the slope in the range between 30-40 which means that this degree does not influence the landslides whereas 50-55 is 4.56 which has higher capability to trigger landslides.

Over all computations helps us understand the influence of each parameter in the landslide event, which will help us to understand the strength and autocorrelation of every parameter in landslides occurrences.

A Python script was written which made the complex process achievable with 5 hours as opposed to the manual process which takes approximately 2 days. Multi-processing techniques were attempted to process tasks in parallel, but *arcpy*'s licensing mechanism prevented running *arcpy* simultaneously within separate processes. Nonetheless, a linear batch processing script was used to effectively automate the analysis of our data.
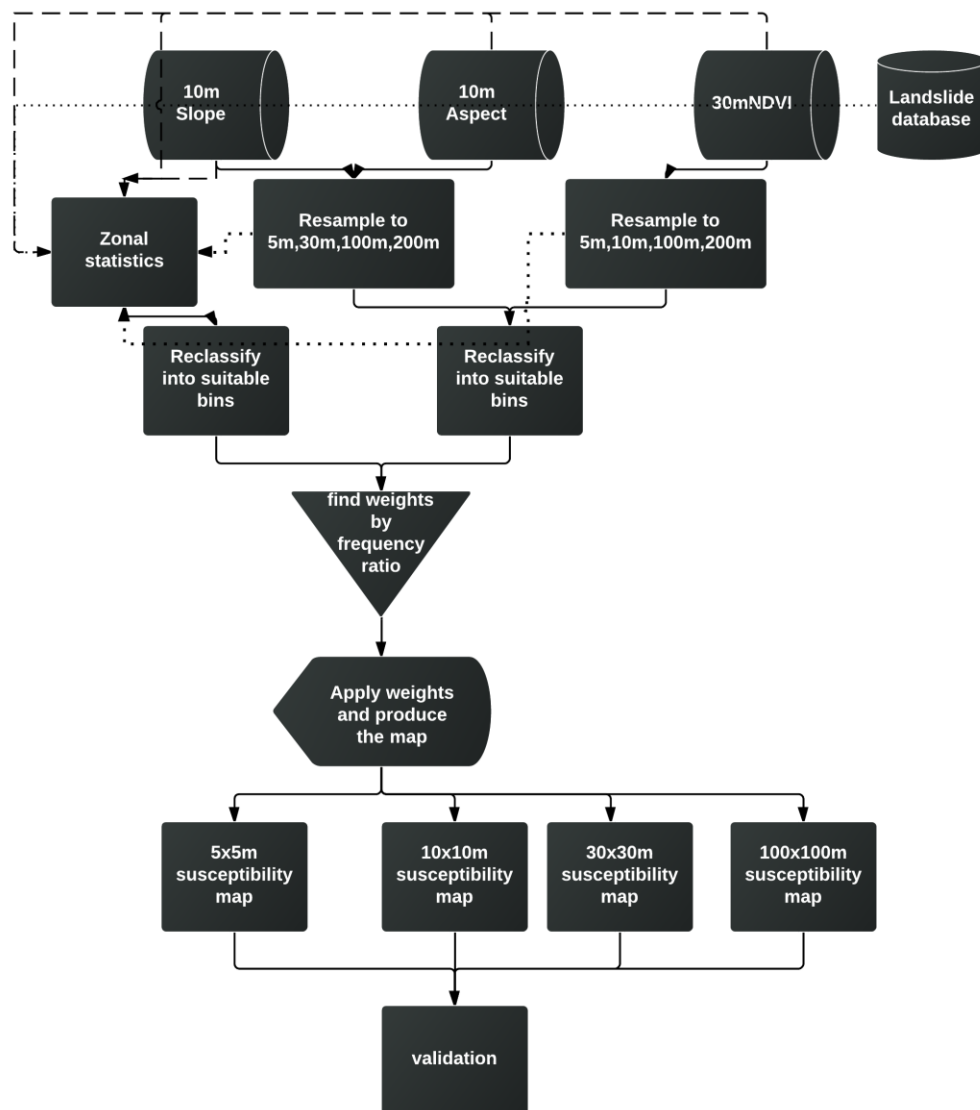
Figure 2 –Methodology of the process

Requirements

Please refer to the read me text associated with the script.

Results and discussion

The following charts show the variation of landslides with different cell sizes. However it is hard to see any variation in slope is very negligible till 65 degree and this is witnessed with the values in the FR table as well. This reflects the fact the much finer resolution is needed in order to find the details. Validation techniques also confirm to the result that cell sizes such as 5, 10 and 30 are closer to accuracy of each other but it is diluted when resolution increases.

Table 1   Frequency ratio of parameter- slope

Bins	Total pixels in the bins (%)				Landslide occuring pixels (%)				Frequency ratio			
	5	10	30	100	5x5m	10x10m	30x30m	100x100m	5x5m	10x10m	30x30m	100x100m
0-5	0.160361	0.19532	0.165791	0.165824	0.068476	0.090345	0.090713	0.098089	0.427009	0.46255	0.547156	0.59152163
5-10	0.214318	0.203062	0.200367	0.200407	0.162589	0.15503	0.152158	0.156003	0.758637	0.763465	0.759393	0.77843319
10-15	0.185692	0.175828	0.177272	0.177227	0.179254	0.169999	0.169375	0.161039	0.965333	0.966847	0.955451	0.90865939
15-20	0.152954	0.145246	0.147469	0.147493	0.16964	0.162515	0.160981	0.159895	1.109095	1.118896	1.091627	1.0840834
20-25	0.118668	0.113403	0.115967	0.115817	0.151907	0.143804	0.14484	0.135058	1.2801	1.26808	1.248976	1.16612698
25-30	0.084025	0.081258	0.085755	0.085867	0.117722	0.11376	0.112881	0.116516	1.401044	1.399983	1.316314	1.35694132
30-35	0.05077	0.050287	0.056915	0.056889	0.080654	0.08222	0.081567	0.083553	1.588614	1.634995	1.433133	1.46869014
35-40	0.023742	0.02465	0.031983	0.032014	0.041983	0.047364	0.051114	0.050589	1.768272	1.921469	1.598176	1.58020895
40-45	0.007578	0.008535	0.013536	0.013527	0.020404	0.024591	0.025395	0.025066	2.692397	2.881172	1.876092	1.8530674
45-50	0.001592	0.001992	0.003957	0.00395	0.005448	0.007377	0.008286	0.010415	3.421641	3.703206	2.094189	2.63703184
50-55	0.000253	0.000348	0.000816	0.000814	0.001496	0.002031	0.001614	0.002632	5.914375	5.831239	1.977991	3.23439235
55-60	3.83E-05	5.61E-05	0.000141	0.00014	0.000427	0.000962	0.000968	0.000687	11.16045	17.14153	6.873514	4.9136293
60-65	7.29E-06	1.04E-05	2.38E-05	2.42E-05			0.000108	0.000343	32.48696	39.09343	4.521878	14.1732484
65-70	1.3E-06	2.24E-06	5.46E-06	5.51E-06				0.000114			26.29389	20.7724329
70-75	3.77E-07	4.9E-07	9.36E-07	7.87E-07								0
75-80	2.3E-07	3.2E-07	4.11E-07	4.37E-07								56.5184672

Table 2   Frequency ratio of parameter- aspect

Bins	Total pixels in the bins (%)				Landslide occuring pixels (%)				Frequency ratio			
	5	10	30	100	5x5m	10x10m	30x30m	100x100m	5x5m	10x10m	30x30m	100x100m
north	0.091613	0.091618	0.126856	0.091524	0.094114	0.094515	0.120198	0.09419709	1.0273	1.031619	0.947514	1.02920183
north-east	0.128953	0.128967	0.12101	0.128967	0.131824	0.132685	0.124718	0.11994964	1.022261	1.02883	1.030638	0.93007803
east	0.13295	0.132949	0.117301	0.132896	0.132037	0.133968	0.126009	0.10941971	0.993131	1.007659	1.074231	0.82334628
south-east	0.135607	0.135619	0.121595	0.135514	0.142827	0.143056	0.136985	0.1141124	1.053241	1.054833	1.126569	0.84206859
south	0.143423	0.14343	0.127862	0.143329	0.14945	0.148936	0.13946	0.15108161	1.042024	1.038386	1.090707	1.05409205
south-west	0.145539	0.145543	0.132653	0.145545	0.141652	0.140383	0.128591	0.15440082	0.973289	0.964548	0.969384	1.06084666
westt	0.134516	0.134514	0.126091	0.13455	0.123705	0.123062	0.113419	0.15028042	0.919629	0.914864	0.8995	1.11690883
north-west	0.0874	0.087359	0.126632	0.087674	0.084393	0.083396	0.110621	0.10655832	0.965596	0.954629	0.87356	1.21539629
									7.996472	7.995368	8.012103	8.07193857

Table3   Frequency ratio of parameter- NDVI

	Total pixels in the bins (%)				Landslide occuring pixels (%)				Frequency ratio			
Bins	5	10	30	100	5x5m	10x10m	30x30m	100x100m	5x5m	10x10m	30x30m	100x100m
-0.9-(-0.8)	1.74E-08	1.74E-08	2.75E-07	1.33E-07	0	0	0	0	0	0	0	0
-0.8-(-0.7)	1.6E-08	1.6E-08	1.01E-07	5.34E-07	0	0	0	0	0	0	0	0
-0.7-(-0.6)	2.74E-08	2.74E-08	2.62E-06	0.000154	0	0	0	0	0	0	0	0
-0.6-(-0.5)	7.76E-07	7.76E-07	0.000271	0.002534	0	0	0	0	0	0	0	0
-0.5-(-0.4)	0.000152	0.000152	0.002742	0.010578	0	0	0	0	0	0	0	0
-0.4-(-0.3)	0.002539	0.002539	0.010734	0.009118	0	0	0	0.000457	0	0	0	0.050136
-0.3-(-0.2)	0.010589	0.010589	0.008906	0.196986	0.000214	0.000214	0.000108	0.002171	0.020185	0.020185	0.012091	0.011023
-0.2-(-0.1)	0.009108	0.009108	0.197967	0.028394	0.001603	0.001603	0.000215	0.005257	0.176015	0.176015	0.001088	0.185151
-0.1-0	0.197042	0.197042	0.029816	0.05049	0.006199	0.006199	0.002046	0.020229	0.031458	0.031458	0.068625	0.400642
0-0.1	0.028374	0.028374	0.051671	0.076404	0.016138	0.016138	0.007754	0.0368	0.568746	0.568746	0.150056	0.481648
0.1-0.2	0.05049	0.05049	0.076029	0.11419	0.037726	0.037726	0.02143	0.063086	0.747198	0.747198	0.281868	0.552465
0.2-0.3	0.076401	0.076401	0.11156	0.142557	0.057176	0.057176	0.04006	0.101943	0.748376	0.748376	0.359092	0.715101
0.3-0.4	0.114146	0.114146	0.138721	0.187258	0.103024	0.103024	0.059552	0.173371	0.902569	0.902569	0.429292	0.925845
0.4-0.5	0.14255	0.14255	0.185938	0.16198	0.171743	0.171743	0.101012	0.266971	1.204791	1.204791	0.543259	1.64817
0.5-0.6	0.187206	0.187206	0.163289	0.019279	0.269745	0.269745	0.166056	0.271429	1.440894	1.440894	1.016948	14.07871
0.6-0.7	0.162027	0.162027	0.022253	7.6e-05	0.273913	0.273913	0.254792	0.058286	1.690537	1.690537	11.44968	767.3955
0.7-0.8	0.019297	0.019297	9.84E-05	6.01E-07	0.06252	0.06252	0.279776		3.239843	3.239843	2843.744	
0.8-0.9	7.7E-05	7.7E-05	1.07E-06					0.067198	0	0	63014.38	
									10.77061	10.77061	65872.43	786.4443
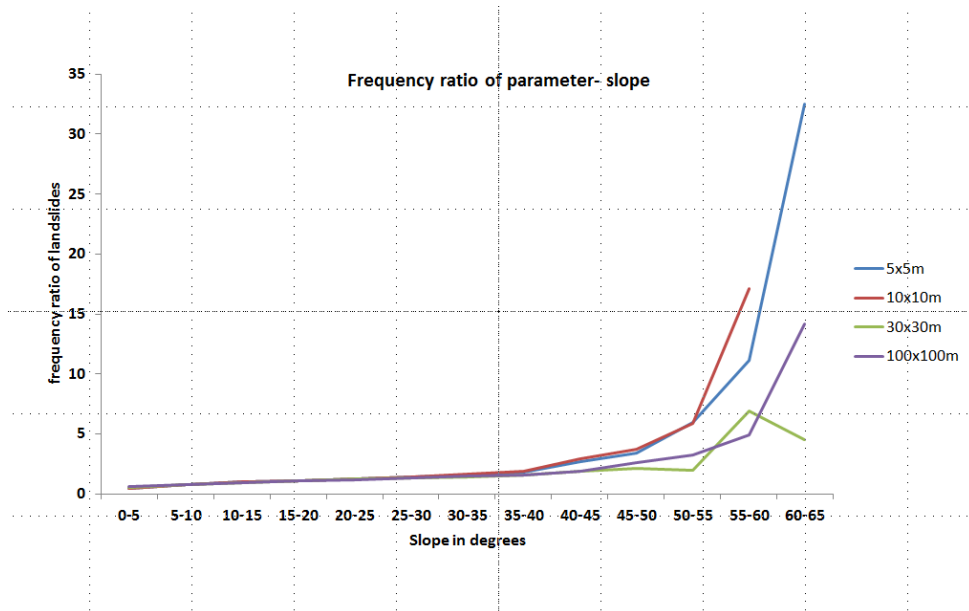
Figure 3
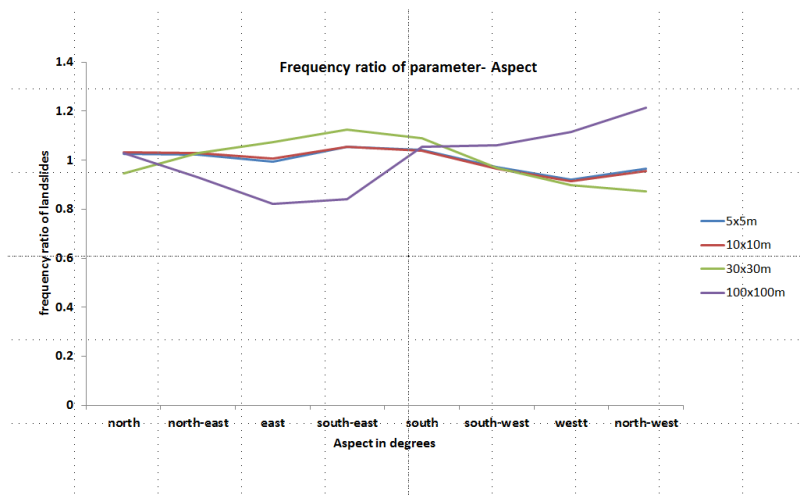
Figure 4
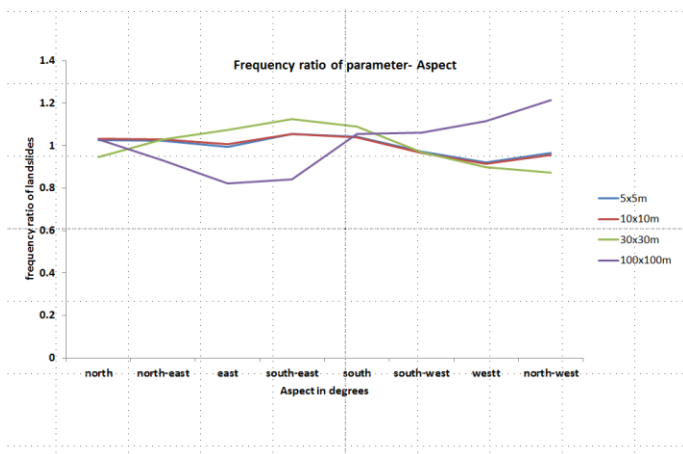
Figure 5
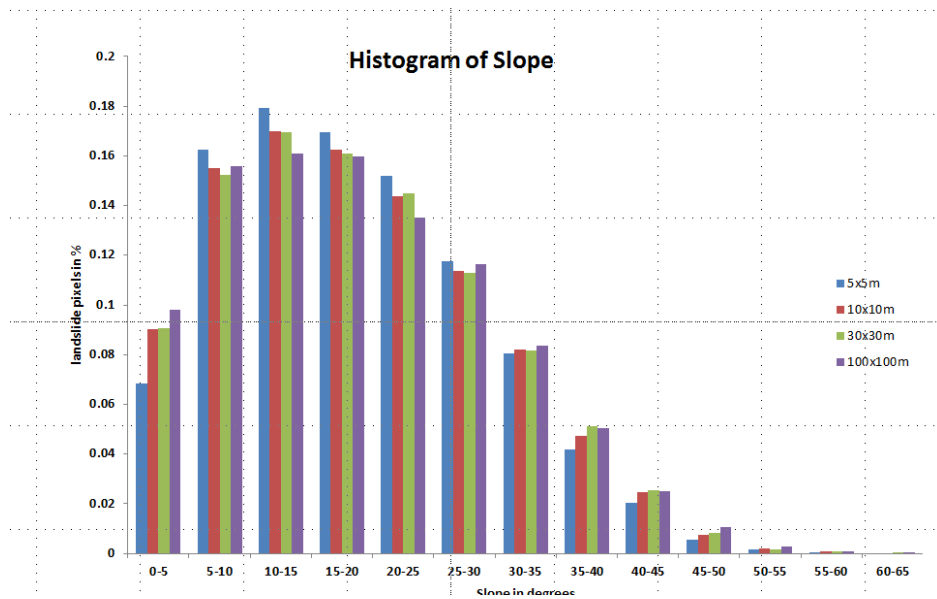
Figure 6

Figure 7

Figure 8

Frequency ratio- probability map (100x100)m

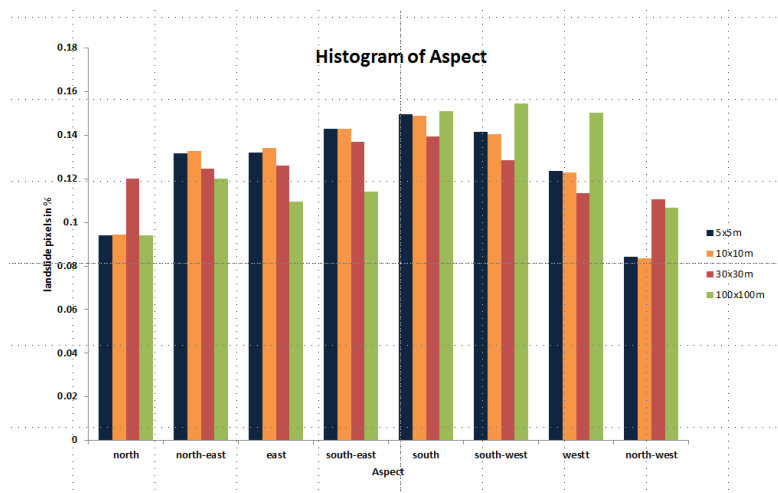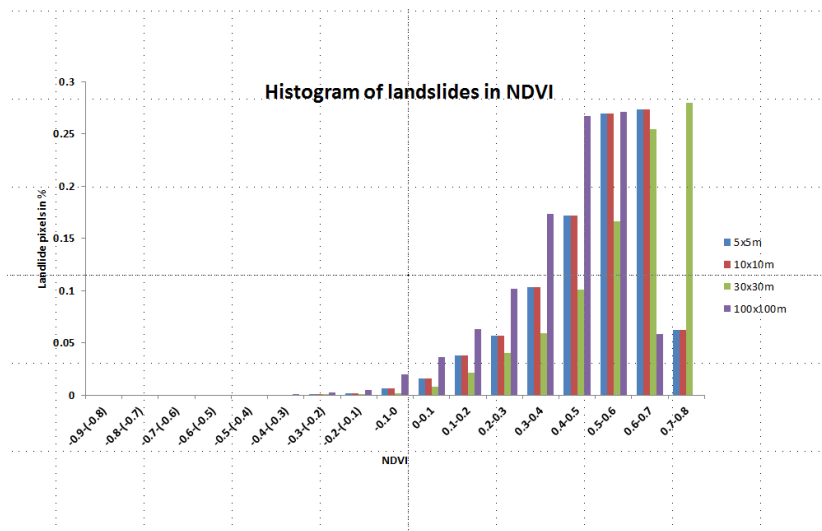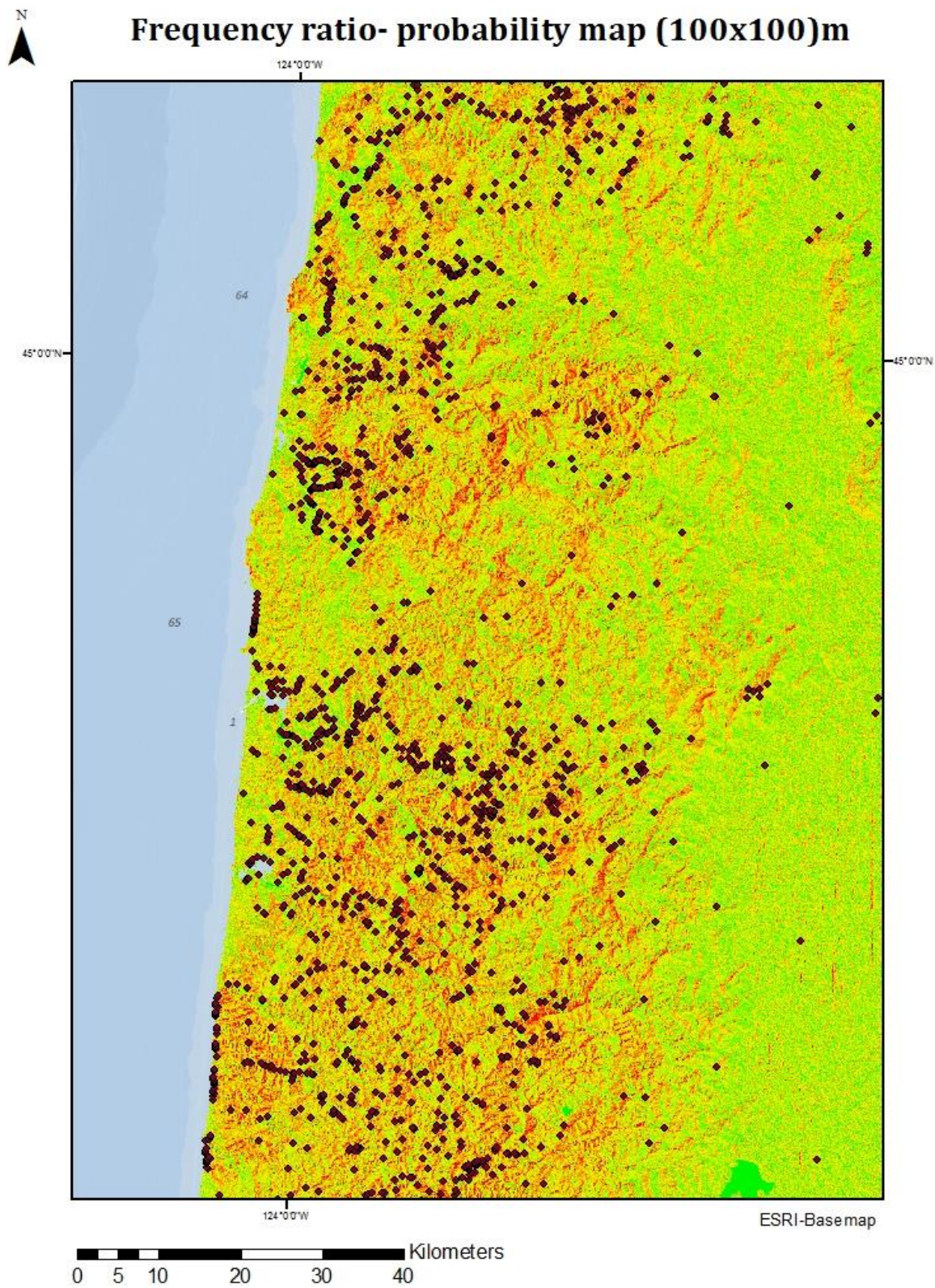**Figure 9**

Various models were used and compared against one another to get the closest accuracy with the available landslides which were initially used to study. And it was found out that 10x10m cell sizes were of the accuracy of 89% which iterates that for a terrain like west coast of Oregon 10m cell sizes would be a good resolution for quality results. However it should be taken in to account that not all the landslide events have been mapped and considered for the analysis. Also not all the parameters mentioned in the generation of the data list is used for this study. However such parameters should be considered following the same methodology and weights be added to compute the susceptibility maps.

In conclusion, LiDAR derived landslides would be best to use for such analysis and also 5m cell sizes was resampled from the original 10m cell size which is averaging and resampling the cell sizes. Better results can be expected when LiDAR DEMs are used because of the fine details in the pixels. FR ratio is well suited for this type of analysis and Python scripting contributed to accelerate the process and minimize the data loss which usually a limitation in other statistical softwares while handling large datasets.

References

Dogami. (2010). Oregon Geology.   Retrieved Aug 2012, from
   http://www.oregongeology.com/sub/learnmore/CoastRange.HTM

GEO, Geospatial Enterprise Office. (2009). Oregon Spatial Data Library. from
   Geospatial Data Clearinghouse
   http://spatialdata.oregonexplorer.info/geoportal/catalog/main/home.page

Guzzetti, F., Carrara, A., Cardinali, M., & Reichenbach, P. (1999). Landslide
   hazard evaluation: a review of current techniques and their application in a
   multi-scale study, Central Italy. *Geomorphology, 31*(1), 181-216.

Guzzetti, F., Reichenbach, P., Cardinali, M., Galli, M., & Ardizzone, F. (2005).
   Probabilistic landslide hazard assessment at the basin scale. *Geomorphology,
   72*(1), 272-299.

Huete, A., Didan, K., Miura, T., Rodriguez, E.P., Gao, X., & Ferreira, L.G. (2002).
   Overview of the radiometric and biophysical performance of the MODIS
   vegetation indices. *Remote sensing of environment, 83*(1), 195-213.

Lee, C.T., Huang, C.C., Lee, J.F., Pan, K.L., Lin, M.L., & Dong, J.J. (2008).
   Statistical approach to earthquake-induced landslide susceptibility.
   Engineering Geology, 100(1), 43-58.

Lee, S., & Min, K. (2001). Statistical analysis of landslide susceptibility at Yongin,
   Korea. *Environmental Geology, 40*(9), 1095-1113.

Lee, S., & Sambath, T. (2006). Landslide susceptibility mapping in the Damrei
   Romel area, Cambodia using frequency ratio and logistic regression models.
   Environmental Geology, 50(6), 847-855.

Lee, Saro, Choi, Jawon, & Woo, Ik. (2004). The effect of spatial resolution on the
   accuracy of landslide susceptibility mapping: a case study in Boun, Korea.
   Geosciences Journal, 8(1), 51-60. doi: 10.1007/BF02910278

Lobo, J.G.R. (2007). *Identifying landslide hazards in a tropical mountain
   environment, using geomorphologic and probabilistic approaches*:
   ProQuest.

Madin, IP, & Burns, WJ. (2006). Map of Landslide Geomorphology of Oregon
   City. *Oregon and Vicinity Interpreted from LIDAR Imagery and Aerial
   Photographs, Oregon Department of Geology and Mineral Industries Open
   File Report O-06-27*.

Marcus, W. A. (2008). A Brief Summary of Oregon Coast Range Geology,
   Geomorphology, Tectonics, and Climate *Geology 4/510: Course notes*:
   University of Oregon.

Nandi, A., & Shakoor, A. (2010). A GIS-based landslide susceptibility evaluation
   using bivariate and multivariate statistical analyses. *Engineering Geology,
   110*(1), 11-20.

William Burns, Ian Madin, Lina Ma, Katherine Mickelson, Evan Saint-Pierre. (2011). *Statewide Landslide Information Database of Oregon Release 2* [ArcGIS vector data].